

## TECHNICAL ADVANCE

# A ubiquitin-10 promoter-based vector set for fluorescent protein tagging facilitates temporal stability and native protein distribution in transient and stable expression studies

Christopher Grefen<sup>1</sup>, Naomi Donald<sup>1</sup>, Kenji Hashimoto<sup>3</sup>, Jörg Kudla<sup>3</sup>, Karin Schumacher<sup>2</sup> and Michael R. Blatt<sup>1,\*</sup>

<sup>1</sup>Laboratory of Plant Physiology and Biophysics, FBLS – Plant Sciences, Bower Building, University of Glasgow, Glasgow G12 8QQ, UK,

<sup>2</sup>Institute for Plant Sciences (HIP), University of Heidelberg, 69120 Heidelberg, Germany, and

<sup>3</sup>Institut für Botanik, Universität Münster, Schlossplatz 4, D48149 Münster, Germany

Received 6 April 2010; revised 14 July 2010; accepted 20 July 2010; published online 8 September 2010.

\*For correspondence (fax +44 (0) 141 330 4447; e-mail m.blatt@bio.gla.ac.uk).

## SUMMARY

Fluorescent tagging of proteins and confocal imaging techniques have become methods of choice in analysing the distributions and dynamic characteristics of proteins at the subcellular level. In common use are a number of strategies for transient expression that greatly reduce the preparation time in advance of imaging, but their applications are limited in success outside a few tractable species and tissues. We previously developed a simple method to transiently express fluorescently-tagged proteins in *Arabidopsis* root epidermis and root hairs. We describe here a set of Gateway-compatible vectors with fluorescent tags incorporating the *ubiquitin-10* gene promoter ( $P_{UBQ10}$ ) of *Arabidopsis* that gives prolonged expression of the fluorescently-tagged proteins, both in tobacco and *Arabidopsis* tissues, after transient transformation, and is equally useful in generating stably transformed lines. As a proof of principle, we carried out transformations with fluorescent markers for the integral plasma membrane protein SYP121, a member of the SNARE family of vesicle-trafficking proteins, and for DHAR1, a cytosolic protein that facilitates the scavenging of reactive oxygen species. We also carried out transformations with SYP121 and its interacting partner, the KC1 K<sup>+</sup> channel, to demonstrate the utility of the methods in bimolecular fluorescence complementation (BiFC). Transient transformations of *Arabidopsis* using *Agrobacterium* co-cultivation methods yielded expression in all epidermal cells, including root hairs and guard cells. Comparative studies showed that the  $P_{UBQ10}$  promoter gives similar levels of expression to that driven by the native SYP121 promoter, faithfully reproducing the characteristics of protein distributions at the subcellular level. Unlike the 35S-driven construct, expression under the  $P_{UBQ10}$  promoter remained elevated for periods in excess of 2 weeks after transient transformation. This toolbox of vectors and fluorescent tags promises significant advantages for the study of membrane dynamics and cellular development, as well as events associated with environmental stimuli in guard cells and nutrient acquisition in roots.

**Keywords:** fluorescent protein fusion construct, root hair, stomatal guard cell, confocal microscopy, bimolecular fluorescence complementation, cell biology.

## INTRODUCTION

The fluorescent tagging of proteins has now become routine in studies of cellular and subcellular localization, since the introduction of GFP and other genetically encoded fluorophores (Chalfie *et al.*, 1994; Heim *et al.*, 1994). In plants,

*Agrobacterium tumefaciens*-mediated gene transfer is the method of choice in generating stable lines of transformed plants carrying the transgene of interest (Herrera-Estrella *et al.*, 1983), and, in recent years, these methods have also

found application in transient transformations. The ability of *Agrobacterium* to transfer T-DNA into plant cells enables the relatively simple approach of infiltrating the bacteria into leaves (Goodin *et al.*, 2002). Leaf infiltrations have found applications in tracing the distribution and dynamics of subcellular compartments (Boevink *et al.*, 1998; Brandizzi *et al.*, 2002; daSilva *et al.*, 2004; Runions *et al.*, 2006), in the analysis of proteins that function in the plant secretory system (Batoko *et al.*, 2000; Geelen *et al.*, 2002; Samalova *et al.*, 2006; Sutter *et al.*, 2006; Tyrrell *et al.*, 2007), and in their interactions *in vivo* (Bracha-Drori *et al.*, 2004; Honsbein *et al.*, 2009). In parallel with localization studies, these methods are now frequently used in preliminary screens for the functional characteristics associated with gene products. Such analyses have included the biophysical and cellular properties of transmembrane ion transporters (Meckel *et al.*, 2004; Sutter *et al.*, 2007; DUBY *et al.*, 2008), the localization and dynamics of trafficking proteins (Foresti *et al.*, 2006; Tyrrell *et al.*, 2007) and the spread of viral pathogens (Baulcombe *et al.*, 1995; Oparka *et al.*, 1999; Haupt *et al.*, 2005).

The strong 35S ( $P_{35S}$ ) promoter of Cauliflower mosaic virus has long been a favoured choice to drive constitutive expression (Benfey and Chua, 1990), both in studies relying on stable and transient transformation. The use of a constitutive promoter has advantages when the gene of interest is normally expressed at low levels, and when tissue-specific characteristics of expression are not of primary concern. However, overexpression can present difficulties of its own, including co-suppression or gene silencing (Elmayan and Vaucheret, 1996; Elmayan *et al.*, 1998; Mishiba *et al.*, 2005), and long-term developmental effects of expressing the gene of interest. Transient expression methods avoid problems associated with development and, at least initially, they circumvent problems of gene silencing, as well as the substantial lead-in time needed to generate transgenic plants. Nonetheless, both stable and transient expression methods can give rise to mislocalisation of target proteins when expressed ectopically at high

levels and, even in transient studies, expression driven by the 35S promoter shows suppression over a period of days (cf. Campanoni *et al.*, 2007).

In search for alternatives we settled on the *Arabidopsis thaliana ubiquitin-10* gene promoter ( $P_{UBQ10}$ ) that facilitates moderate expression in nearly all tissues of *Arabidopsis* (Norris *et al.*, 1993). We developed a vector set that combines the advantages of previous systems using the  $P_{UBQ10}$  promoter (Geldner *et al.*, 2009), adding the advantages of Gateway compatibility for fast and efficient cloning, the ease of selection using Basta and hygromycin resistance in stable lines, and incorporates the option to generate both N- and C-terminal fusion constructs for expression. The latter option is especially important, as N- or C-terminal fusions can mask the targeting sequences of proteins and lead to mis-localisation of the fusion protein product. Thus, it is a standard requirement to prepare and test fusion constructs in both configurations. Finally, we extended recent methods for transient expression based on co-cultivation of *Agrobacterium* with *Arabidopsis* seedlings (Campanoni *et al.*, 2007; Li *et al.*, 2009). Here, we describe applications of the  $P_{UBQ10}$ -based vector set in generating fluorescent fusion proteins, and their application to expression in *Arabidopsis* in stable lines, and after co-cultivation in *Arabidopsis* and tobacco. We show that the vector set gives moderate levels of expression of intrinsic membrane and soluble proteins, both in tobacco and *Arabidopsis*, but with a temporal stability after transient transformation that is apparently limited only by the maintenance of the plants. We report, too, that these transient methods enable reliable transformation of guard cells as well as epidermal cells and root hairs in *Arabidopsis*.

## RESULTS AND DISCUSSION

The Gateway-compatible, pUB-Dest vector set (Figure 1; see also Figure S1) was designed to enable both N- and C-terminal fusions of proteins of interest with several fluorophores, including eGFP, mRFP, CFP and YFP (Fricker *et al.*, 2006), the bimolecular fluorescence complementation (BiFC) components nYFP\* and cYFP (Walter *et al.*, 2004), as well as

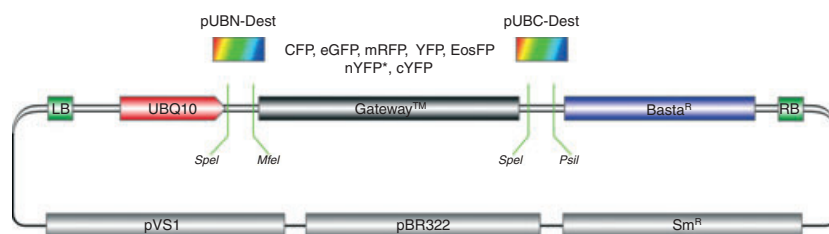


**Figure 1.** Schematic representation of the pUB-Dest vector series. N-terminal fusion tags were introduced using *SpeI/MfeI*, and C-terminal fusion tags were introduced using *SpeI/PstI*. The expression cassette is under the control of the *Arabidopsis* ubiquitin-10 promoter (At4g05320; 634 bp immediately preceding the ATG start codon) and contains a 3' polyadenylation signal (not depicted). In addition, the T-DNA carries the gene phosphinothricin-*N*-acetyltransferase that confers resistance to the herbicide Basta (nYFP\* constructs carry resistance to the antibiotic hygromycin) embedded in 5'- and 3'-regulatory elements of the nopaline synthase. The vector backbone contains the pVS replication sequence for maintenance in *Agrobacterium tumefaciens*, the pBR322 origin for high copy number in *Escherichia coli*, and the aminoglycoside-3-adenyltransferase gene for resistance against streptomycin or spectinomycin in bacteria.

the photoconvertible EOS fluorescent protein (Wiedenmann *et al.*, 2004; Gurskaya *et al.*, 2006). These binary vectors incorporated the nucleotide sequence corresponding to the first 634 base pairs of the promoter ( $P_{UBQ10}$ ) immediately upstream of the *ubiquitin-10* gene from *Arabidopsis* (*At4g05320*). They also included sequences encoding phosphinothricin-*N*-acetyltransferase and aminoglycoside-3-adenyltransferase for resistance to Basta or hygromycin in the plant, and to streptomycin and spectinomycin in *Escherichia coli*, respectively.

To determine the efficiency of transformation and to characterize expression, we made use both of immunological methods and confocal laser scanning microscopy. The analysis was based in part on comparative measurements with the same vectors incorporating the standard 35S ( $P_{35S}$ ) promoter, both in tobacco and in *Arabidopsis* after transient transformations. For this purpose we used two markers: (i) the *Arabidopsis* SNARE protein SYP121 (*At3g11820*; 38 kDa), an integral plasma membrane protein that is known to express throughout the plant (Lipka *et al.*, 2007; Bassham and Blatt, 2008; Enami *et al.*, 2009), and overlaps functionally with its tobacco homologue (Sutter *et al.*, 2006); and (ii) the *Arabidopsis* dehydroascorbate reductase DHAR1 (*At1g19570*; 24 kDa), a redoxin that is found primarily in the cytosol, but has also been associated with membranes (Dixon *et al.*, 2002; Elter *et al.*, 2007). We also carried out analyses using BiFC constructs of SYP121 and its interacting partner, the  $K^+$  channel KC1 (*At4g32650*; 78 kDa) (Honsbein *et al.*, 2009). As described below, the analysis also summarizes standardized parameters for co-cultivation of *Arabidopsis* with *Agrobacterium tumefaciens* GV3101 that give consistent and prolonged expression of fusion proteins in root, hypocotyl, shoot, and cotyledon epidermis, as well as in guard cells of *Arabidopsis* seedlings.

#### Agrobacterium growth and transgene expression

Bacterial preparation proved an important determinant for the efficient transformation and expression, both of tobacco and *Arabidopsis*. We compared the relative efficiency of transformation with *Agrobacterium tumefaciens* harvested from liquid culture following a single 16-h growth cycle (Campanoni *et al.*, 2007), and following a subculture cycle for an additional 6–8-h period after the bacteria were diluted 1:10 in fresh medium, following the method of Grefen *et al.* (2008), before harvesting (final  $OD_{600}$ , 1–2). After harvest and pre-treatment with acetosyringone, *Agrobacterium* carrying DHAR1 and SYP121 fusion constructs were infiltrated into tobacco leaves and co-cultivated with 4-day-old *Arabidopsis* seedlings in half-strength MS salts plus 0.003% Sylwet, as described previously (Campanoni *et al.*, 2007; Li *et al.*, 2009). The concentration of *Agrobacterium* used for injections and in co-cultivation proved to have no measurable effect on transformation efficiency, whereas increasing the pH of the co-cultivation medium, especially, promoted transformation

and expression, much as we reported previously for *Agrobacterium rhizogenes*-mediated transformation (Campanoni *et al.*, 2007); by contrast, the fluorescence signals were enhanced between three- and five-fold when the bacteria were passed through the additional subculture cycle (Grefen *et al.*, 2008), and we therefore standardized conditions, based on this method, with a final  $OD_{600}$  of 0.2 and pH of 7 that yielded over 90% transformation efficiency of *Arabidopsis* with *Agrobacterium tumefaciens*.

#### Yield and temporal characteristics of $P_{UBQ10}$ -driven expression

Differences associated with the  $P_{35S}$  and  $P_{UBQ10}$  promoters were most notable in construct expression in tobacco. Quantified on the basis of fluorescence yield, leaf infiltrations of tobacco with *Agrobacterium* carrying the SYP121-GFP construct gave roughly 20-fold greater signal driven by the  $P_{35S}$  promoter compared with the same construct under  $P_{UBQ10}$  control (Figures 2a and 3); however, this difference in fluorescence signals was greatly attenuated when expressed in *Arabidopsis* (Figure 2a). The difference between tobacco and *Arabidopsis* expression was confirmed by western blot analysis showing the presence of the doublet of bands (Geelen *et al.*, 2002; Tyrrell *et al.*, 2007), recognized by polyclonal antibodies to SYP121 (Figure 2c). Expressed under both promoters, the vesicle trafficking protein showed a strong fluorescence associated with the cell periphery (Figure 3), consistent with its known localization to the plasma membrane where it facilitates the final stages of membrane fusion between vesicle and target membranes (Lipka *et al.*, 2007; Bassham and Blatt, 2008), as well as controlling channel-mediated  $K^+$  transport (Honsbein *et al.*, 2009). We noted in every case the absence of any appreciable fluorescence from internal structures with  $P_{UBQ10}$ -driven expression. Expressed under the  $P_{35S}$  promoter, SYP121-GFP fluorescence was frequently associated with mobile punctate structures in the cytosol (Figure 3a–d; see also Video Clips S1, S2 and S3) and, occasionally, with the nucleus in tobacco. These latter observations are consistent with retention in the secretory pathway (Campanoni *et al.*, 2007), and may indicate the formation of inclusion bodies associated with the high levels of  $P_{35S}$ -driven expression. This interpretation was supported by fluorescence bleaching experiments that showed a pronounced mobility of SYP121 fluorescence within cells when expressed under the control of the  $P_{35S}$  promoter, but not under  $P_{UBQ10}$  control (not shown; see Figure 5 below).

The SYP121 construct exhibited prolonged transgene expression that remained substantially elevated even 2 weeks after transformation, both in tobacco and *Arabidopsis*, when driven by the  $P_{UBQ10}$  promoter. Under our standardized conditions, the fluorescence yield for SYP121-GFP reached a maximum, independent of the promoter, approximately 72 h after adding the bacteria.

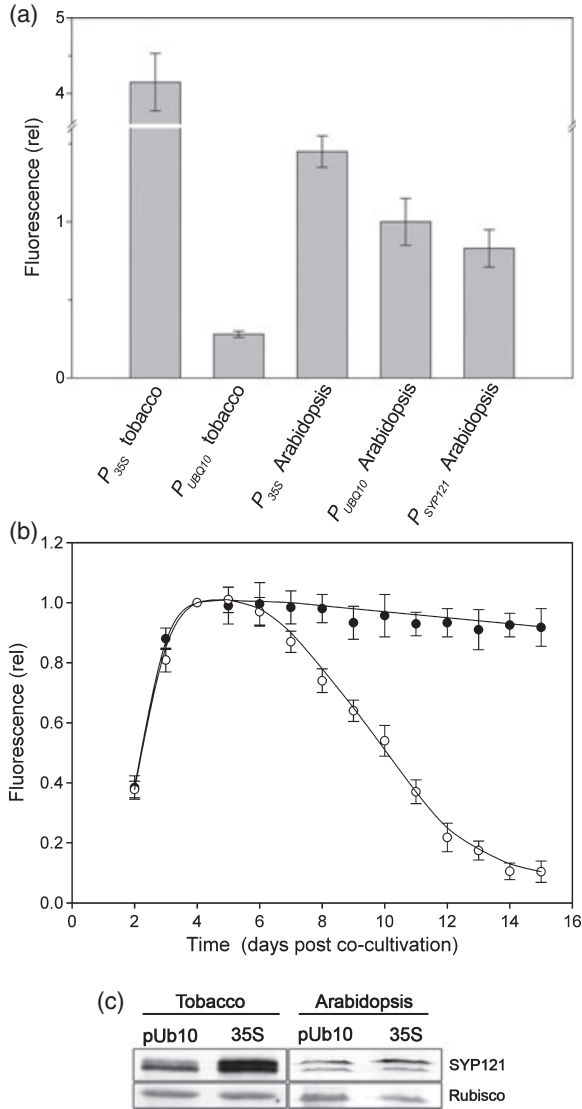


**Figure 2.** Moderated expression of the plasma membrane marker SYP121-GFP by the  $P_{UBQ10}$  promoter. Relative fluorescence yields from tobacco leaves and Arabidopsis roots expressing SYP121-GFP driven by the  $P_{UBQ10}$  and  $P_{35S}$  promoters. Data in each case from three separate cycles of transformations and 18 randomly selected image sets taken with standardized settings 4 days after infiltration (tobacco) and co-cultivation (Arabidopsis) with *Agrobacterium* harvested after subculturing. Data for Arabidopsis stably expressing SYP121-GFP under the control of its own promoter (Pajonk *et al.*, 2008) are included for comparison. (B) Relative fluorescence from Arabidopsis roots expressing SYP121-GFP driven by the  $P_{UBQ10}$  (●) and  $P_{35S}$  (○) promoters as a function of days after co-cultivation. Data are from three separate cycles of transformations and 18 randomly selected image sets taken with standardized settings, as in (A), and are normalized to the mean fluorescence signals for day 4. Similar patterns of expression were obtained for tobacco (not shown). (C) Western blot analysis of SYP121-GFP expression driven by  $P_{UBQ10}$  and  $P_{35S}$  promoters in tobacco and Arabidopsis. Tissue samples taken 4 days after infiltration (tobacco) and co-cultivation (Arabidopsis). Each lane corresponds to 5  $\mu\text{g ml}^{-1}$  of total protein. Ponceau loading control with a protein band of Rubisco is shown below in each case. Similar results were obtained in two separate experiments.

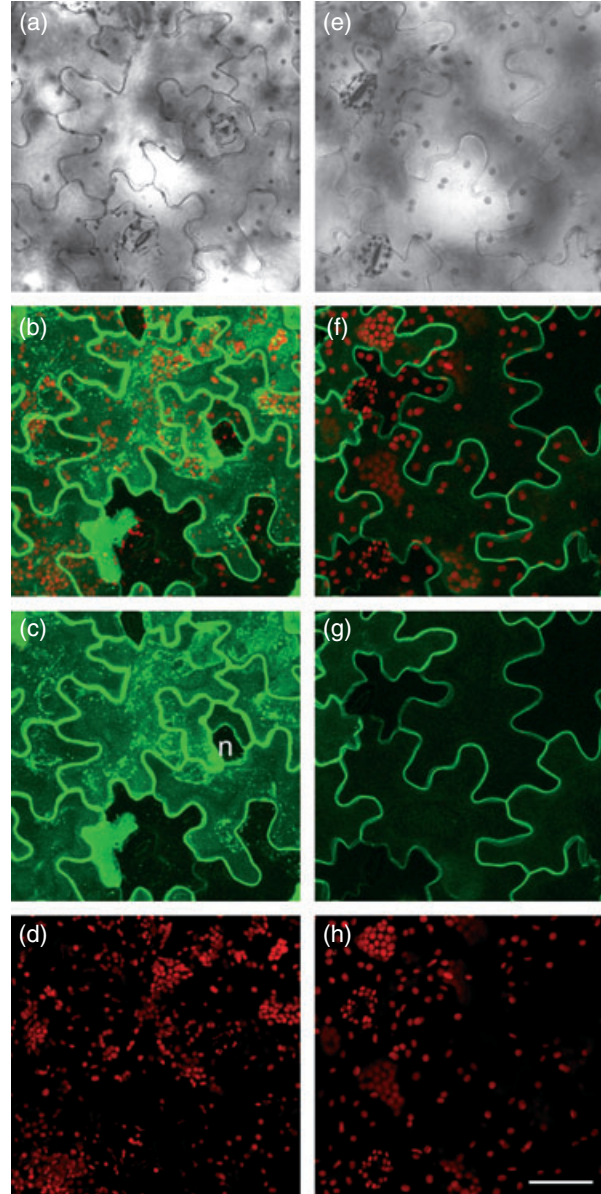


**Figure 3.** Moderated expression of the plasma membrane marker SYP121-GFP by the  $P_{UBQ10}$  promoter labels only the plasma membrane in tobacco epidermal cells. Comparison of GFP fluorescence from tobacco leaves, 3 days post-infiltration with *Agrobacterium tumefaciens* carrying SYP121-GFP driven by the Cauliflower mosaic virus  $P_{35S}$  promoter (a–d) and by the  $P_{UBQ10}$  promoter (e–h). Identical emission settings were used to collect GFP fluorescence. Excitation at 488 nm was attenuated 10-fold for images (a–d). Frames (b–d) and (f–h) are three-dimensional image projections reconstructed from image stacks (see also Video Clips S1 and S2); frames are brightfield (a, e), composite fluorescence (b, f), GFP fluorescence (c, g) and chloroplast fluorescence (d, h). Inclusion structures (visible in frames b and c) and a fluorescent ring around the nucleus (n, in frame c) were frequently evident on expression driven by the  $P_{35S}$  promoter, but were never evident under  $P_{UBQ10}$ -driven expression. See also Video Clips S3. Scale bar: 50  $\mu\text{m}$ .

Expression remained essentially stable thereafter for the  $P_{UBQ10}$ -driven construct, but decayed significantly after 6–8 days when driven by the  $P_{35S}$  promoter, whether

expressed in Arabidopsis (Figure 2c) or in tobacco (not shown). Analysis of DHAR1-GFP expression led to a similar conclusion. Finally, we noted that SYP121-GFP fluorescence under  $P_{UBQ10}$  control compared favourably with that of the SYP121 transgene when stably expressed and driven by its own promoter ( $P_{SYP121}$  Figure 2A; see also Figures 4–7), although transcriptional analyses (see Figure S2; Winter *et al.*, 2007) suggest a 5–10-fold enhancement would be expected with the  $P_{UBQ10}$ -driven construct. Indeed, translational and post-translational factors are likely to contribute to the temporal characteristics of transgene expression (Grefen *et al.*, 2008). Thus, the similarity in fluorescence yields in this case is fortuitous. Nonetheless, we suspect that the moderate activity of the  $P_{UBQ10}$ -driven system means that its control of expression is less prone to gene silencing over time.

#### Cellular characteristics of $P_{UBQ10}$ -driven expression

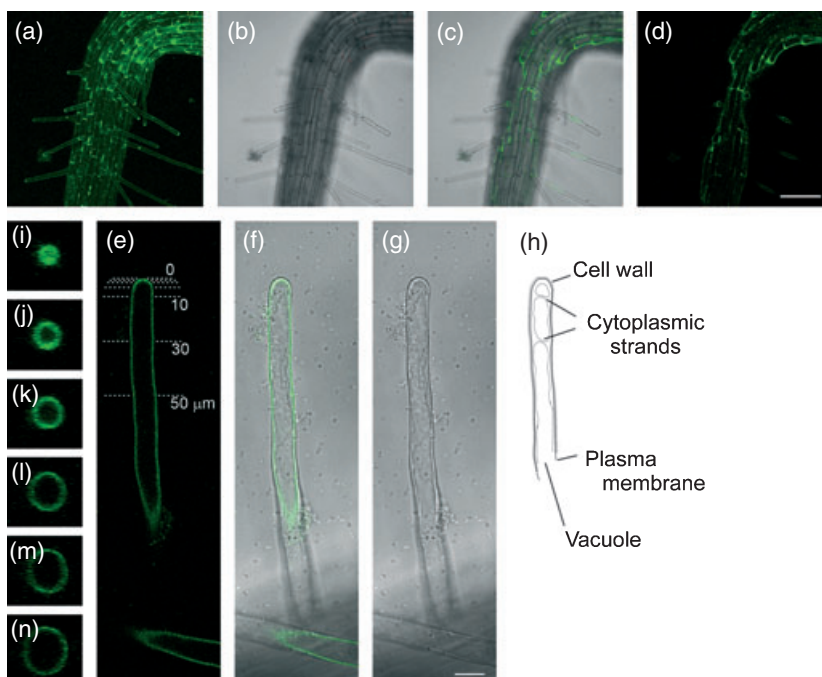
Co-cultivation of Arabidopsis seedlings and *Agrobacterium* with T-DNA carrying fluorescent transgene fusions invariably led to the transformation of the root tissues, hypocotyl, stem and cotyledons. Within these tissues, transformation was limited to the outer (epidermal) cell layer, much as was reported previously (Campanoni *et al.*, 2007), indicating that all cells exposed to the *Agrobacterium* culture during co-cultivation are subject to transformation. Figure 4 illustrates results typical of transformations with  $P_{UBQ10}$ -driven SYP121-GFP and its distribution in the root epidermis, as well as the advantages for confocal image analysis of expression in a tissue that shows little or no background fluorescence. Driven by the  $P_{UBQ10}$  promoter, SYP121-GFP

fluorescence was observed along the length of the root, both in epidermal cell files forming root hairs (trichoblasts) and those that did not (atrachoblasts). SYP121-GFP fluorescence was strongest, however, at the base of trichoblasts and at the tips of root hairs, especially younger – presumably still growing – root hairs (see Figure 4a–d; Video Clip S4). Analysis of individual root hairs (Figure 4e–n) showed the fluorescence to be associated with the cell periphery, not with the cytosol or tonoplast, and we noted the absence of any appreciable fluorescence from internal structures. Furthermore, SYP121 showed little evidence of mobility within individual root hairs, consistent with its situation as an integral plasma membrane protein. In the latter case, we used fluorescence recovery after photobleaching (FRAP) and fluorescence lifetime in photobleaching (FLIP) experiments to assess lateral movement of SYP121-GFP when expressed in root hairs, and we repeated these measurements with experiments using SYP121-EOS to follow the dynamics of the SNARE after photoactivation of the photochromic EOS protein (Figure 5).

Using fluorescence yield, we compared the  $P_{UBQ10}$ -driven expression of SYP121 with that of the SNARE when stably expressed and driven by its own promoter ( $P_{SYP121}$ ). Under  $P_{SYP121}$  control, SYP121-GFP expression has been reported throughout the vegetative plant, especially in epidermal tissues of leaves, stems, the root and root hairs (Enami *et al.*, 2009). Within the root epidermis and root hairs, we found the  $P_{UBQ10}$  promoter to faithfully reproduce the protein distribution, with expression driven by the  $SYP121$  promoter (Figure 6A). In each case, the fluorophore tag was strongest at the basal end of trichoblasts and at the tips of younger root hairs

**Figure 4.**  $P_{UBQ10}$ -driven expression of SYP121-GFP in Arabidopsis root epidermis shows GFP fluorescence polarized to the base of trichoblast cells and to the tips of root hairs.

Low magnification images (a–d) of one root 4 days after co-cultivation as a three-dimensional reconstruction of the image stack (a), mid-plane brightfield (b), mid-plane brightfield and GFP fluorescence overlay (c), and mid-plane GFP fluorescence (d) images (see also Video Clips S4). Scale bar: 100  $\mu$ m. High-magnification images (e–n) of a single root hair in longitudinal section as GFP fluorescence (e), fluorescence and brightfield composite (f), and brightfield (g) shows fluorescence restricted to the cell periphery, not the cytosolic strands or tonoplast [compare schematic (h) on right]. Radial optical sections at the root hair tip (i) and at distances from the tip of 0.5 (j), 1 (k), 5 (l), 10 (m) and 30  $\mu$ m (n), reconstructed from a three-dimensional image stack of the root hair [section positions indicated in (e)]. Scale bar: 10  $\mu$ m (e–h); 5  $\mu$ m (i–n).



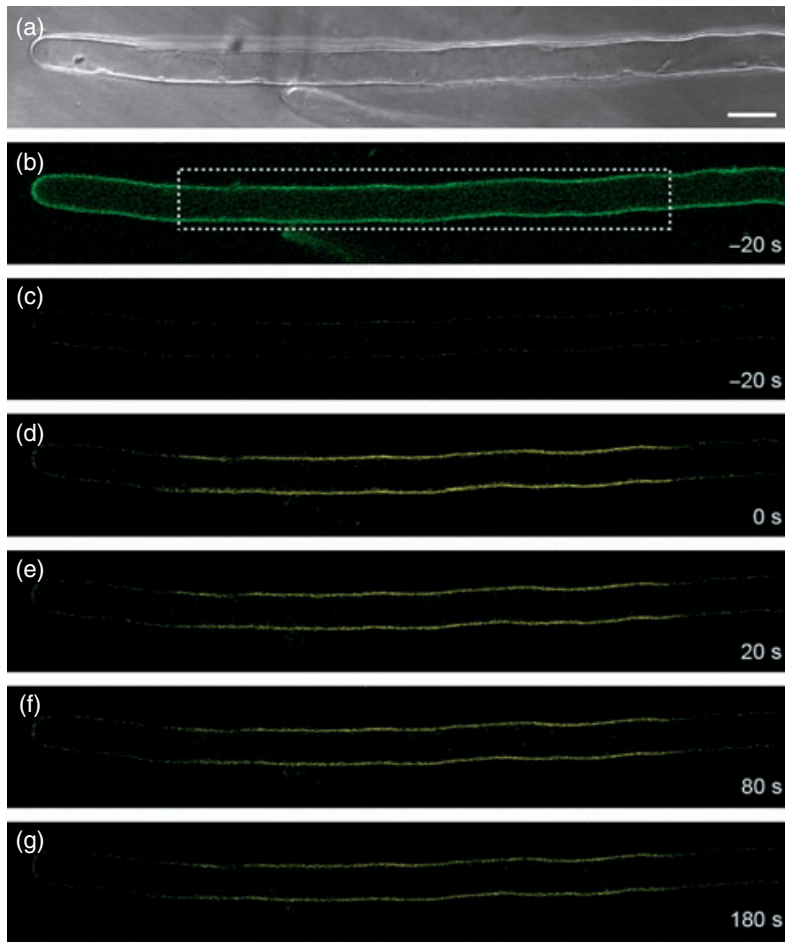


**Figure 5.** Transient  $P_{UBQ10}$ -driven expression of SYP121-EOS in the root hair of an Arabidopsis seedling after 3 days co-cultivation. EOS photoconversion was with 351- and 364-nm light in the boxed area indicated in frame (b). Frames show brightfield (a), EOS fluorescence collected at 505–530 nm after excitation with 488-nm light before photoconversion (b), and EOS fluorescence collected at 580–615 nm on excitation with 543-nm light (b–g) before and after photoconversion (times indicated on the right relative to the end of photoconversion at time zero). Note the stable localization of EOS fluorescence to the photoactivated region of the root hair.

(Figure 6B; see also Figure 4a–d,i–n). We noted a pronounced elevation in fluorescence around the dome of the root hair that dropped off steeply within the first 10–20  $\mu\text{m}$  of the tip apex (Figure 6b,c). Quantified on the basis of peripheral fluorescence at the apex relative to the base of the root hair, SYP121 showed the greatest difference in its distribution in root hairs shorter than 40–60  $\mu\text{m}$ , with the fluorescence ratio declining to approximately 2:1 in root hairs longer than 140–160  $\mu\text{m}$ , irrespective of the promoter driving expression (Figure 6a). The same distribution was reflected in YFP fluorescence following  $P_{UBQ10}$ -driven expression of the BiFC partners fused with SYP121 with the  $\text{K}^+$  channel subunit KC1 (Figure S3; Video Clip S8). This enhanced localization to the root hair tip suggests a corresponding spatial distribution to the channel and SNARE functionalities, and may bear on their roles in  $\text{K}^+$  nutrition (Honsbein *et al.*, 2009).

Finally, it is of particular interest that our use of the  $P_{UBQ10}$  promoter and the strategies based on co-cultivation also lead to transient transformation of stomatal guard cells in Arabidopsis. In the past, studies of protein dynamics in guard cells have been hampered by the recalcitrance of this cell type to transient transformation by *Agrobacterium*, leaving biolistic methods as the only alternative (Meckel

*et al.*, 2005; Mikosch *et al.*, 2006; Sutter *et al.*, 2007). Figure 7 shows DHAR1-EOS expressed in epidermal and guard cells of an Arabidopsis cotyledon, and compares favourably with DHAR1-EOS expressed stably in Arabidopsis (not shown) when driven by the  $P_{UBQ10}$  promoter. Images were taken before and after photoactivation of the EOS protein, and they clearly show the local rise in EOS emission at wavelengths of 560–615 nm, with excitation at 543 nm following photoactivation, and its spread within those cells targeted in photoactivation. Also visible is a concurrent decline in emission between 505 and 530 nm, with excitation at 488 nm, that is a common feature of EOS photoactivation (Wiedenmann *et al.*, 2004). DHAR1 is predominantly a cytosolic protein like other members of the redoxin/GST transferase protein family (Noctor and Foyer, 1998; Frova, 2006), so its mobility within the cell is expected. The EOS photoconversion in this case offers a check against interference from background fluorescence associated with these photosynthetic tissues, as chloroplast fluorescence is also enhanced by the high-intensity light used in photoconversion. The observations thus underscore the utility of the transformation strategy in studies of protein dynamics in guard cells, for example in relation to environmental stimuli.

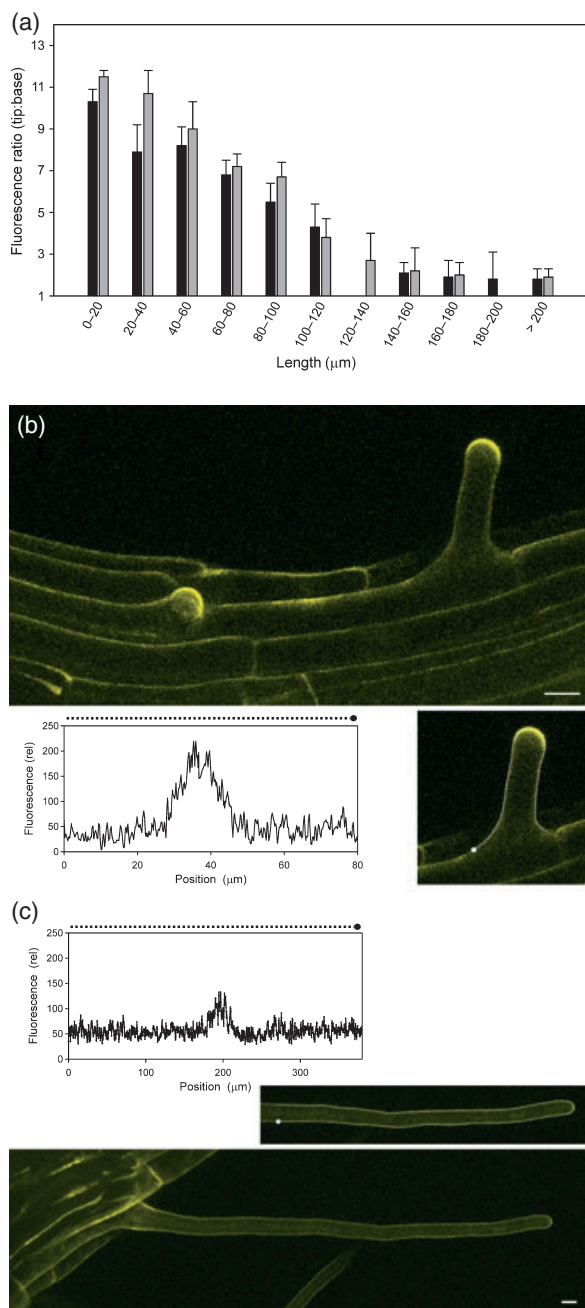


**Figure 6.** Fluorescence signals of SYP121-YFP driven by the SYP121 promoter in a stably transformed line of Arabidopsis (Pajonk *et al.*, 2008) and of  $P_{UBQ10}$ -driven SYP121-GFP shows fluorescence polarized to the base of trichoblast cells and to the tips of root hairs.

(A) Mean tip: base fluorescence ratio decays with the developmental age of Arabidopsis root hairs. Ratios determined from the peripheral fluorescence signals of three-dimensional images of the apical dome to 5 μm behind the tip, and of the epidermal cell base of the root hair, such as shown in (B) and (C) below, and plotted as a function of root hair length. Data are means ± SEs from at least eight root hairs in each case for stable transgenic Arabidopsis expressing SYP121-YFP driven by the native  $P_{SYP121}$  promoter (black bars), and for Arabidopsis co-cultivated with *Agrobacterium*, and expressing SYP121-GFP under the control of the  $P_{UBQ10}$  promoter (grey bars).

(B) Three-dimensional reconstruction of stably-expressed SYP121-YFP fluorescence from one image stack showing the polarized YFP fluorescence associated with a young root hair and root hair initial (see also Video Clips S5). Scale bar: 10 μm. Insets (below): relative fluorescence as a function of position around the root hair periphery. Mean fluorescence plotted from a 3-pixel-wide line around the root hair (right). Position indicated by dotted line and lollipop above plot. Similar examples of fluorescence distribution with  $P_{UBQ10}$ -driven SYP121-GFP expression can be found in Figures 4 and S3.

(C) Three-dimensional projections of stably-expressed SYP121-YFP fluorescence from one image stack showing the polarized YFP fluorescence associated with a mature root hair (see also Video Clips S6). Scale bar: 10 μm. Insets (above): relative fluorescence as a function of position around the root hair periphery. Mean fluorescence plotted from a 3-pixel-wide line around the root hair (right). Position indicated by dotted line and circle above plot. Similar examples of fluorescence distribution with  $P_{UBQ10}$ -driven SYP121-GFP expression can be found in Figures 4 and S3.

promoter gives exceptional temporal stability that, in conjunction with a co-cultivation strategy, enables reliable transformation of guard cells as well as epidermal cells and root hairs in Arabidopsis. These tools should find wide application in studies, for example, of polar development, root–rhizosphere interactions, ion transport and interactions with symbionts, and may also find applications in high-throughput screens directed to characterizing candidate gene products and their partners.

## EXPERIMENTAL PROCEDURES

### Vector construction

A 634 bp genomic DNA fragment immediately upstream of the ATG start codon was identified, based on the UBQ10 promoter sequence (Norris *et al.*, 1993) and was amplified from Arabidopsis Col-6 genomic DNA using forward (5'-gccaagcttGTCGACGAGTCAGTAATAACG-3') and reverse (5'-gcgctcgagCTGTTAATCAGAAAACTCAG-3') primers. The amplified fragment was digested by *Hind*III and *Xho*I and cloned into pGPTVII.GFP (Walter *et al.*, 2004) to verify its ability to drive GFP expression after *Agrobacterium*-mediated transformation in *Nicotiana benthamiana*. Sequencing of several clones showed a C to A nucleotide exchange at position -29 in the Col-6 promoter sequence when compared to that of the published Col-0 sequence (Norris *et al.*, 1993). The promoter was introduced into the pUGT1 vector (K. Schumacher, unpublished) from which it was excised as a starting point in developing the vectors described here.

The vector pB7WGR2 (Karimi *et al.*, 2002) was digested using *Spe*I and *Afl*II, and the opened segment amplified by PCR using a forward primer generating 5' *Spe*I and *Psi*I sites upstream of the T35S, and a 3' *Afl*II site to incorporate the Basta resistance gene (see Figure S1 for details). Ligation of this PCR product into the open vector created an intermediate construct. The 35S promoter was

In conclusion, we present an improved vector set for transformation, as well as extended methods for transient expression analysis in Arabidopsis. These new tools will help accelerate studies of endosomal organization, protein localization and dynamics, and will facilitate work on root hairs and in guard cells that, in the past, have proven recalcitrant to transient *Agrobacterium*-mediated transformation as a strategy for transient gene expression. Our vector set offers straightforward access to both N- and C-terminal fusion constructs with a promoter that gives moderate levels of expression of both intrinsic membrane and soluble proteins. Expression based on the  $P_{UBQ10}$

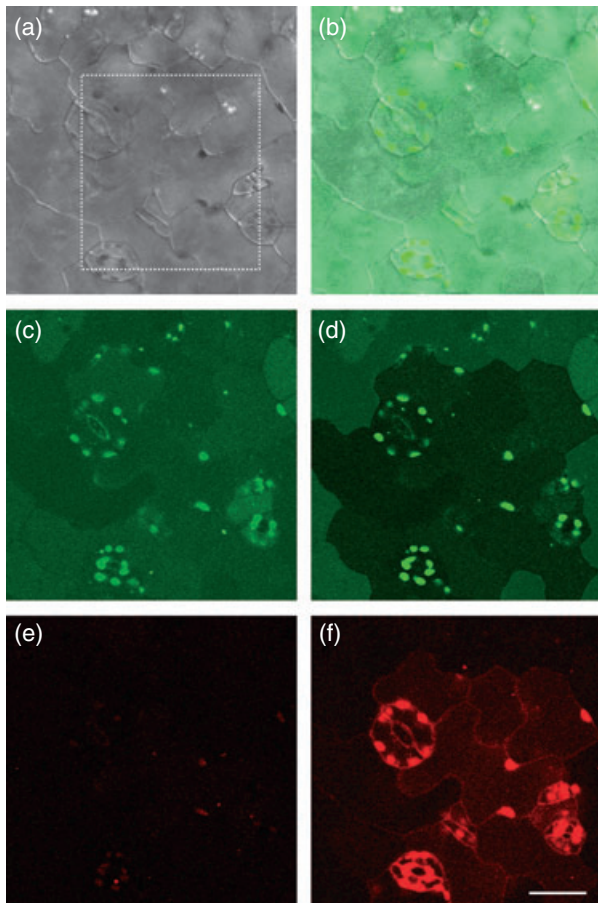


**Figure 7.** Transgene expression in the cotyledon epidermis and guard cells of *Arabidopsis* seedlings after co-cultivation with *Agrobacterium*.

Brightfield (a), composite (b) and EOS fluorescence (c) images of the cotyledon epidermis of an *Arabidopsis* seedling expressing DHAR1-EOS under the control of the  $P_{UBQ10}$  promoter 3 days after co-cultivation. EOS fluorescence collected at 505–530 nm after excitation with 488-nm light before (c) and after (d) EOS photoconversion with 351 and 364 nm light within the area indicated by the dotted box in frame (a). EOS fluorescence collected concurrently at 580–615 nm after excitation with 543-nm light before (e) and after (f) EOS photoconversion. Note the DHAR1-EOS fluorescence appearing in all cells transected by the 351/364-nm photoconversion light. Light at 351/364 nm also enhances chloroplast fluorescence. Scale bar: 50  $\mu\text{m}$ . See Video Clips S7 for a complete time series of DHAR1-EOS fluorescence photoconversion.

removed by digestion with *PmeI* and *SpeI*, and was replaced with a corresponding fragment from the vector pUGT1, containing the UBQ10 promoter followed by the Gateway cassette, thereby creating pUB-Dest. Fluorescence tags mGFP6, mYFP, mRFP and EOS, as well as the split-YFP variants nYFP and cYFP (Walter *et al.*, 2004; Wiedenmann *et al.*, 2004; Fricker *et al.*, 2006), were synthesized via PCR to introduce 5' *SpeI* and 3' *PsiI* sites, and were subsequently ligated into the vector creating the C-terminal vector set in pUBC-Dest.

To generate the corresponding vector set with N-terminal fluorophores, two PCR fragments were created, using pUB-Dest as a template. The fragments contained the vector backbone, the first stretching from an *AvrII* site between the pVS replication and pBR322 origin to the 3' end of the UBQ10 promoter, adding *SpeI* and *MfeI* sites, and a second stretching from the *AvrII* site to the 5' end of

the 35S terminator, and adding *MfeI* and *PsiI* sites. Ligation of these fragments resulted in a circular vector lacking a Gateway cassette. This intermediate vector was opened using the blunt end enzyme *PsiI* and the Gateway cassette A from the Gateway Conversion kit (Invitrogen, <http://www.invitrogen.com>) was introduced, creating the pUBN-Dest vector. The fluorescence tags were amplified by PCR to introduce *SpeI* and *MfeI* sites at the 5' and 3' ends, respectively, and were ligated into pUBN-Dest to generate the N-terminal vector set. A schematic of both pUBN-Dest and pUBC-Dest is shown in Figure 1.

### Gateway cloning and bacterial transformation

All Gateway vectors were cloned and amplified using *E. coli* *ccdB*-survival<sup>TM</sup> cells (Invitrogen), and selected using spectinomycin (100  $\mu\text{g ml}^{-1}$ ) and chloramphenicol (30  $\mu\text{g ml}^{-1}$ ). Vector backbones were verified by restriction digest analysis and complete sequencing. Entry clones encoding SYP121, KC1 and DHAR1 were constructed by PCR amplification using primers that contained attB1 and attB2 sites as 5' modifications. Gel-purified PCR products were introduced into pDONR207 (Invitrogen) using BP-clonase II according to the manufacturer's instructions. Recombinant entry clones were amplified in Top10<sup>TM</sup> cells (Invitrogen), and were verified by restriction digest analysis and sequencing. LR recombination reactions were performed by mixing 1  $\mu\text{l}$  (=150 ng) of pUBC-Dest or pUBN-Dest vector, including the fluorophores, 1  $\mu\text{l}$  (=150 ng) of the entry clone and 0.5  $\mu\text{l}$  of LR-clonase II (Invitrogen) to generate SYP121 and DHAR1 N-terminally and KC1 C-terminally tagged with the fluorophores. The reaction was incubated at room temperature (20°C) for 1 h. Aliquots of 1  $\mu\text{l}$  were then used to transform Top10 bacterial cells, which were grown overnight at 37°C on 2% agar plates with Luria Bertani (LB) media containing 100  $\mu\text{g ml}^{-1}$  spectinomycin. Selected colonies were isolated and the clones were verified through restriction digest analysis. Destination clones were transformed subsequently in *Agrobacterium tumefaciens* strain GV3101 pMP90 (Koncz and Schell, 1986). Successful transformations were verified by plasmid rescue in *E. coli* and restriction digest analysis.

### Plant transformation

*Agrobacterium* carrying clones of interest were grown in a first cycle overnight (16 h, 220 rpm, 28°C) in 5 ml LB medium with 50  $\mu\text{g ml}^{-1}$  rifampicin, 25  $\mu\text{g ml}^{-1}$  gentamycin and 100  $\mu\text{g ml}^{-1}$  spectinomycin. A second cycle of growth was started by inoculating an aliquot from the overnight growth at a 1:10 dilution in fresh medium, and then cultured for 6–8 h (220 rpm, 28°C) to give a final OD<sub>600</sub> of 1–2. The bacteria were harvested and resuspended in 10 mM MgCl<sub>2</sub> with 150  $\mu\text{M}$  acetosyringone (3,5-dimethoxy-acetophenone; Fluka, now part of Sigma-Aldrich, <http://www.sigmaaldrich.com>) and 10 mM 2-(*N*-morpholine)-ethanesulphonic acid (MES), pH 5.5, before dilution in the same medium to give a final OD<sub>600</sub> 0.1 or 0.2 for tobacco leaf infiltration. For co-cultivation with *Arabidopsis*, the bacteria were resuspended in half-strength MS basal salts medium (Sigma-Aldrich), pH 7, to a final OD<sub>600</sub> 0.2–0.3 with 150  $\mu\text{M}$  acetosyringone and 0.003% Sylwet-77 (Lehle Seeds, <http://www.arabidopsis.com>) (Campanoni *et al.*, 2007; Li *et al.*, 2009).

### Plant material and co-cultivation

*Nicotiana benthamiana* and *Nicotiana tabacum* were grown as described previously (Sutter *et al.*, 2006). *A. thaliana* L. (ecotype Columbia) seeds were sterilized for 10 min in 10% NaHClO<sub>3</sub> with 1% Triton-X100 and stratified at least 2 days at 4°C in the dark before incubation in six-well plates containing 3 ml half-strength MS medium. *Arabidopsis* seeds were germinated under constant light

at 80  $\mu\text{mol s}^{-1} \text{m}^{-2}$  light and 22°C. After germination, the medium was exchanged with fresh half-strength MS plus 150  $\mu\text{M}$  acetosyringone, 0.003% Sylwet-77, including a suspension of *Agrobacterium* carrying the transgene of interest.

### Confocal microscopy and quantification

Expression was determined by confocal laser imaging, using a Carl Zeiss CLSM510-META-UV confocal laser scanning microscope (Carl Zeiss, Inc., <http://www.zeiss.co.uk>), with argon ion and helium/neon lasers. For visualizing GFP and non-photoactivated EOS, excitation at 488 nm was used and fluorescence collected after reflection off an NFT545 dichroic mirror and passage through a 505–530-nm bandpass filter. EOS was photoactivated with 351- and 364-nm light from an Enterprise II UV laser, and the photoactivated EOS was visualized with excitation at 543 nm after passage through an NFT545 dichroic mirror and 560–615-nm bandpass filter. Chloroplast fluorescence was separated using a CFT635 dichroic mirror and was collected using the META detector set for a bandwidth of 632–700 nm. Laser power, dichroics, filters, detector gains and offsets were kept fixed for all the different specimens, to allow comparison between the different samples. As necessary, only the laser attenuation was varied within the pre-calibrated linear range of the tuneable optical filters of the instrument. Transformation, distributions and fluorescence tracking were quantified using both the Carl Zeiss LSM 510 AIM software (v3.2) and IMAGEJ (<http://www.rsweb.nih.gov/ij>). Fluorescence values are reported as the means  $\pm$  SEs of at least three independent experiments or 18 seedlings after subtracting background fluorescence measured in controls co-cultivated with non-transformed *Agrobacterium*.

### Total protein extraction and western blot analysis

For expression analysis by western blot, seedlings were harvested after examination under the confocal microscope, flash-frozen and ground under liquid nitrogen. Total proteins were extracted in denaturing 'lyse and load' buffer (50 mM Tris-HCl, pH 6.8, 4% sodium dodecylsulfate, 8 M urea, 30% glycerol, 0.1 M dithiothreitol and 0.005% bromophenol blue), and SDS-PAGE and western blot analyses were performed as described previously (Grefen *et al.*, 2009). Polyclonal rabbit anti-GFP primary antibody (Abcam, <http://www.abcam.com>) was diluted 1:5000. Bound antibodies were detected using goat, anti-rabbit IgG alkaline phosphatase (Sigma-Aldrich) and staining solution of 66  $\mu\text{l}$  MBT (50 mg  $\text{ml}^{-1}$  nitro-blue-tetrazolium chloride in 70% dimethylformamide) and 33  $\mu\text{l}$  BCIP (50 mg  $\text{ml}^{-1}$  5-bromo-4-chloro-3-indolylphosphate-*p*-toluidine in 100% dimethylformamide) in 10 ml of staining buffer containing 100 mM Tris-HCl, pH 9.5, 100 mM NaCl and 5 mM  $\text{MgCl}_2$ .

### Material requests

All non-commercial vector constructs described in this article are available for academic and non-profit use on request.

### ACKNOWLEDGEMENTS

We are grateful to Amparo Ruiz-Pardo for help in the glasshouse, and to Annegret Honsbein for comments on the manuscript. This work was supported by grants BB/F001630/1 and BB/F001673/1 from the UK Biotechnology and Biological Sciences Research Council and a VIP Award grant from the Wellcome Trust to MRB, and by grants from the DFG (FOR 964) to KS and JK.

### SUPPORTING INFORMATION

Additional Supporting Information may be found in the online version of this article:

**Figure S1.** Cloning strategies used to construct the pUBC-Dest (A) and pUBN-Dest (B) vectors. Details of vector construction are provided in Experimental procedures.

**Figure S2.** Analysis of *UBQ10* gene expression (red bars), and its comparison with the markers *SYP121* (blue bars), *DHAR1* (yellow bars) and *KC1* (green bars) used in this study, and the common housekeeping reference gene, *ACT2* (actin 2, white bars). Data expressed as arbitrary units (above) and as the  $\log_2$  fold change (below) relative to a TGT value of 100, as obtained for the tissues indicated from the eFP Browser (Winter *et al.*, 2007).

**Figure S3.** Transient expression in an *Arabidopsis* seedling of the bimolecular fluorescence complementation (BiFC) pair SYP121-cYFP and KC1-nYFP. Brightfield (a) and three-dimensional projection (b) of YFP fluorescence recovered from the assembled YFP moiety shows the pronounced association of the SNARE and  $\text{K}^+$  channel proteins near the base of trichoblasts and tips of young root hairs (see also Video Clip S8). Scale bar: 20  $\mu\text{m}$ .

**Video Clip S1.** GFP fluorescence from tobacco leaves, 3-days post-infiltration with *Agrobacterium* carrying SYP121-GFP driven by the Cauliflower mosaic virus *P*<sub>35S</sub> promoter. Chloroplast fluorescence overlay in red. Note the inclusion structures and fluorescent rings around the nuclei. See Figure 3 legend for details.

**Video Clip S2.** GFP fluorescence from tobacco leaves, 3 days post-infiltration with *Agrobacterium* carrying SYP121-GFP driven by the *P*<sub>UBQ10</sub> promoter. Chloroplast fluorescence overlay in red. See Figure 3 legend for details.

**Video Clip S3.** 35S-driven expression of SYP121-GFP in tobacco epidermis at high magnification shows GFP fluorescence localized to highly-mobile punctate structures that are visible moving within and around the cell periphery, and in cytoplasmic strands. Note that the large (5–7  $\mu\text{m}$ ) fluorescent structures are chloroplasts. These organelles emit both in the GFP channel (pseudo-colour coded green) and at longer wavelengths (pseudo-colour coded red). Elapsed time indicated at top right. Scale bar: 10  $\mu\text{m}$ .

**Video Clip S4.** *P*<sub>UBQ10</sub>-driven expression of SYP121-GFP in *Arabidopsis* root epidermis shows GFP fluorescence polarized to the base of trichoblast cells and to the tips of root hairs. See Figure 4 for details.

**Video Clip S5.** Three-dimensional reconstruction of SYP121-YFP expression driven by the *P*<sub>SYP121</sub> promoter in a stably transformed line of *Arabidopsis* (Pajonk *et al.*, 2008) shows fluorescence polarized to the base of trichoblast cells and to the tips of a young root hair and root hair initial. See Figure 6 for details.

**Video Clip S6.** Three-dimensional reconstruction of SYP121-YFP expression driven by the *P*<sub>SYP121</sub> promoter in a stably transformed line of *Arabidopsis* (Pajonk *et al.*, 2008) shows fluorescence polarized to the base of trichoblast cells and to the tips of a mature root hair. See Figure 6 for details.

**Video Clip S7.** Transgene expression in the cotyledon epidermis and guard cells of *Arabidopsis* seedlings after co-cultivation with *Agrobacterium* showing the time course of DHAR1-EOS photoconversion to emission at 580–615 nm on excitation with 543-nm light. Photoconversion driven by 2- $\mu\text{s}$  exposures to 351- and 364-nm light repeated between each frame, beginning after time  $t = 0$ , as indicated. See Figure 7 for details.

**Video Clip S8.** Three-dimensional reconstruction of *P*<sub>UBQ10</sub>-driven transient expression in an *Arabidopsis* seedling of the bimolecular fluorescence complementation (BiFC) pair SYP121-cYFP and KC1-nYFP. See Figure S3 for details.

Please note: As a service to our authors and readers, this journal provides Supporting Information supplied by the authors. Such materials are peer-reviewed and may be re-organized for online delivery, but are not copy-edited or typeset. Technical support

issues arising from supporting information (other than missing files) should be addressed to the authors.

## REFERENCES

- Bassham, D.C. and Blatt, M.R. (2008) SNAREs – cogs or coordinators in signalling and development? *Plant Physiol.* **147**, 1504–1515.
- Batoko, H., Zheng, H.Q., Hawes, C. and Moore, I. (2000) A Rab1 GTPase is required for transport between the endoplasmic reticulum and Golgi apparatus and for normal Golgi movement in plants. *Plant Cell*, **12**, 2201–2217.
- Baulcombe, D.C., Chapman, S. and Cruz, S.S. (1995) Jellyfish green fluorescent protein as a reporter for virus-infections. *Plant J.* **7**, 1045–1053.
- Benfey, P.N. and Chua, N.H. (1990) The Cauliflower Mosaic Virus 35S promoter – combinatorial regulation of transcription in plants. *Science*, **250**, 959–966.
- Boevink, P., Oparka, K., Cruz, S.S., Martin, B., Betteridge, A. and Hawes, C. (1998) Stacks on tracks: the plant Golgi apparatus traffics on an actin/ER network. *Plant J.* **15**, 441–447.
- Bracha-Drori, K., Shichrur, K., Katz, A., Oliva, M., Angelovici, R., Yalovsky, S. and Ohad, N. (2004) Detection of protein-protein interactions in plants using bimolecular fluorescence complementation. *Plant J.* **40**, 419–427.
- Brandizzi, F., Snapp, E.L., Roberts, A.G., Lippincott-Schwartz, J. and Hawes, C. (2002) Membrane protein transport between the endoplasmic reticulum and the golgi in tobacco leaves is energy dependent but cytoskeleton independent: evidence from selective photobleaching. *Plant Cell*, **14**, 1293–1309.
- Campanoni, P., Sutter, J.-U., Craig, S., Littlejohn, G. and Blatt, M.R. (2007) A generalized method for transfecting root epidermis uncovers endosomal dynamics in Arabidopsis root hairs. *Plant J.* **51**, 322–330.
- Chalfie, M., Tu, Y., Euskirchen, G., Ward, W.W. and Prasher, D.C. (1994) Green Fluorescent Protein as a marker for gene expression. *Science*, **263**, 802–805.
- Dixon, D.P., Davis, B.G. and Edwards, R. (2002) Functional divergence in the glutathione transferase superfamily in plants – Identification of two classes with putative functions in redox homeostasis in *Arabidopsis thaliana*. *J. Biol. Chem.* **277**, 30859–30869.
- Duby, G., Hosy, E., Fzimes, C., Alcon, C., Costa, A., Sentenac, H. and Thibaud, J.B. (2008) AtKC1, a conditionally targeted Shaker-type subunit, regulates the activity of plant K<sup>+</sup> channels. *Plant J.* **53**, 115–123.
- Elmayan, T. and Vaucheret, H. (1996) Expression of single copies of a strongly expressed 35S transgene can be silenced post-transcriptionally. *Plant J.* **9**, 787–797.
- Elmayan, T., Balzerque, S., Beon, F. et al. (1998) Arabidopsis mutants impaired in cosuppression. *Plant Cell*, **10**, 1747–1757.
- Elter, A., Hartel, A., Sieben, C., Hertel, B., Fischer-Schliebs, E., Luttgé, U., Moroni, A. and Thiel, G. (2007) A plant homolog of animal chloride intracellular channels (CLICs) generates an ion conductance in heterologous systems. *J. Biol. Chem.* **282**, 8786–8792.
- Enami, K., Ichikawa, M., Uemura, T., Kutsuna, N., Hasezawa, S., Nakagawa, T., Nakano, A. and Sato, M.H. (2009) Differential expression control and polarized distribution of plasma membrane-resident SYP1 SNAREs in *Arabidopsis thaliana*. *Plant Cell Physiol.* **50**, 280–289.
- Foresti, O., daSilva, L.L.P. and Denecke, J. (2006) Overexpression of the *Arabidopsis* syntaxin PEP12/SYP21 inhibits transport from the prevacuolar compartment to the lytic vacuole *in vivo*. *Plant Cell*, **18**, 2275–2293.
- Fricke, M.D., Runions, J. and Moore, I. (2006) Quantitative fluorescence microscopy: from art to science. *Annu. Rev. Plant Biol.* **57**, 79–107.
- Frova, C. (2006) Glutathione transferases in the genomics era: new insights and perspectives. *Biomol. Eng.* **23**, 149–169.
- Geelen, D., Leyman, B., Batoko, H., Di Sansabastiano, G.P., Moore, I. and Blatt, M.R. (2002) The abscisic acid-related SNARE homolog NtSyr1 contributes to secretion and growth: evidence from competition with its cytosolic domain. *Plant Cell*, **14**, 387–406.
- Geldner, N., ervaud-Tendon, V., Hyman, D.L., Mayer, U., Stierhof, Y.D. and Chory, J. (2009) Rapid, combinatorial analysis of membrane compartments in intact plants with a multicolor marker set. *Plant J.* **59**, 169–178.
- Goodin, M.M., Dietzgen, R.G., Schichnes, D., Ruzin, S. and Jackson, A.O. (2002) pGD vectors: versatile tools for the expression of green and red fluorescent protein fusions in agroinfiltrated plant leaves. *Plant J.* **31**, 375–383.
- Grefen, C., Stadele, K., Ruzicka, K., Obrdlik, P., Harter, K. and Horak, J. (2008) Subcellular localization and *in vivo* interactions of the *Arabidopsis thaliana* ethylene receptor family members. *Mol. Plant*, **1**, 308–320.
- Grefen, C., Obrdlik, P. and Harter, K. (2009) The determination of protein-protein interactions by the mating-based split-ubiquitin system (mbSUS). *Methods Mol. Biol.* **479**, 1–17.
- Gurskaya, N.G., Verkhusha, V.V., Shcheglov, A.S., Staroverov, D.B., Chepurnykh, T.V., Fradkov, A.F., Lukyanov, S. and Lukyanov, K.A. (2006) Engineering of a monomeric green-to-red photoactivatable fluorescent protein induced by blue light. *Nat. Biotechnol.* **24**, 461–465.
- Haupt, S., Cowan, G.H., Ziegler, A., Roberts, A.G., Oparka, K.J. and Torrance, L. (2005) Two plant-viral movement proteins traffic in the endocytic recycling pathway. *Plant Cell*, **17**, 164–181.
- Heim, R., Prasher, D.C. and Tsien, R.Y. (1994) Wavelength mutations and posttranslational autooxidation of Green Fluorescent Protein. *Proc. Natl Acad. Sci. USA*, **91**, 12501–12504.
- Herreraestrella, L., Depicker, A., VanMontagu, M. and Schell, J. (1983) Expression of chimaeric genes transferred into plant cells using a Ti-plasmid-derived vector. *Nature*, **303**, 209–213.
- Honsbein, A., Campanoni, P., Sokolovski, S., Pratelli, R., Chen, Z., Paneque-Corralles, M., Johansson, I. and Blatt, M.R. (2009) A tripartite SNARE-K<sup>+</sup> channel complex mediates channel-dependent K<sup>+</sup> nutrition in Arabidopsis. *Plant Cell*, **21**, 2859–2877.
- Karimi, M., Inze, D. and Depicker, A. (2002) GATEWAY vectors for *Agrobacterium*-mediated plant transformation. *Trends Plant Sci.* **7**, 193–195.
- Koncz, C. and Schell, J. (1986) The promoter of TL-DNA gene 5 controls the tissue-specific expression of chimeric genes carried by a novel type of *Agrobacterium* binary vector. *Mol. Gen. Genet.* **204**, 383–396.
- Li, J.F., Park, E., von Arnim, A.G. and Nebenfuhr, A. (2009) The FAST technique: a simplified *Agrobacterium*-based transformation method for transient gene expression analysis in seedlings of Arabidopsis and other plant species. *Plant Methods*, **5**, DOI 10.1186/1746-4811-5-6.
- Lipka, V., Kwon, C. and Panstruga, R. (2007) SNARE-Ware: the role of SNARE-Domain proteins in plant biology. *Annu. Rev. Cell Dev. Biol.* **23**, 147–174.
- Meckel, T., Hurst, A.C., Thiel, G. and Homann, U. (2004) Endocytosis against high turgor: intact guard cells of *Vicia faba* constitutively endocytose fluorescently labelled plasma membrane and GFP-tagged K<sup>+</sup>-channel KAT1. *Plant J.* **39**, 182–193.
- Meckel, T., Hurst, A.C., Thiel, G. and Homann, U. (2005) Guard cells undergo constitutive and pressure-driven membrane turnover. *Protoplasma*, **226**, 23–29.
- Mikosch, M., Hurst, A.C., Hertel, B. and Homann, U. (2006) Diacidic motif is required for efficient transport of the K<sup>+</sup> channel KAT1 to the plasma membrane. *Plant Physiol.* **142**, 923–930.
- Mishiba, K., Nishihara, M., Nakatsuka, T., Abe, Y., Hirano, H., Yokoi, T., Kikuchi, A. and Yamamura, S. (2005) Consistent transcriptional silencing of 35S-driven transgenes in gentian. *Plant J.* **44**, 541–556.
- Noctor, G. and Foyer, C.H. (1998) Ascorbate and glutathione: keeping active oxygen under control. *Annu. Rev. Plant Physiol. Plant Mol. Biol.* **49**, 249–279.
- Norris, S.R., Meyer, S.E. and Callis, J. (1993) The intron of *Arabidopsis thaliana* polyubiquitin genes is conserved in location and is a quantitative determinant of chimeric gene expression. *Plant Mol. Biol.* **21**, 895–906.
- Oparka, K.J., Roberts, A.G., Boevink, P., Santacruz, S., Roberts, L., Pradel, K.S., Imlau, A., Kotlizky, G., Sauer, N. and Epel, B. (1999) Simple, but not branched, plasmodesmata allow the nonspecific trafficking of proteins in developing tobacco leaves. *Cell*, **97**, 743–754.
- Pajonk, S., Kwon, C., Clemens, N., Panstruga, R. and Schulze-Lefert, P. (2008) Activity determinants and functional specialization of Arabidopsis PEN1 syntaxin in innate immunity. *J. Biol. Chem.* **283**, 26974–26984.
- Runions, J., Brach, T., Kuhner, S. and Hawes, C. (2006) Photoactivation of GFP reveals protein dynamics within the endoplasmic reticulum membrane. *J. Exp. Bot.* **57**, 43–50.
- Samalova, M., Fricker, M. and Moore, I. (2006) Ratiometric fluorescence-imaging assays of plant membrane traffic using polyproteins. *Traffic*, **7**, 1701–1723.
- daSilva, L.L.P., Snapp, E.L., Denecke, J., Lippincott-Schwartz, J., Hawes, C. and Brandizzi, F. (2004) Endoplasmic reticulum export sites and golgi bodies behave as single mobile secretory units in plant cells. *Plant Cell*, **16**, 1753–1771.

- Sutter, J.U., Campanoni, P., Tyrrell, M. and Blatt, M.R.** (2006) Selective mobility and sensitivity to SNAREs is exhibited by the Arabidopsis KAT1 K<sup>+</sup> channel at the plasma membrane. *Plant Cell*, **18**, 935–954.
- Sutter, J.U., Sieben, C., Hartel, A., Eisenach, C., Thiel, G. and Blatt, M.R.** (2007) Abscisic acid triggers the endocytosis of the Arabidopsis KAT1 K<sup>+</sup> channel and its recycling to the plasma membrane. *Curr. Biol.* **17**, 1396–1402.
- Tyrrell, M., Campanoni, P., Sutter, J.-U., Pratelli, R., Paneque-Corralles, M. and Blatt, M.R.** (2007) Selective targeting of plasma membrane and tonoplast traffic by inhibitory (dominant-negative) SNARE fragments. *Plant J.* **51**, 1099–1115.
- Walter, M., Chaban, C., Schutze, K. et al.** (2004) Visualization of protein interactions in living plant cells using bimolecular fluorescence complementation. *Plant J.* **40**, 428–438.
- Wiedenmann, J., Ivanchenko, S., Oswald, F., Schmitt, F., Rocker, C., Salih, A., Spindler, K.D. and Nienhaus, G.U.** (2004) EosFP, a fluorescent marker protein with UV-inducible green-to-red fluorescence conversion. *Proc. Natl Acad. Sci. USA*, **101**, 15905–15910.
- Winter, D., Vinegar, B., Nahal, H., Ammar, R., Wilson, G.V. and Provart, N.J.** (2007) An “electronic fluorescent pictograph” browser for exploring and analyzing large-scale biological data sets. *PLoS ONE*, **2**, e718. doi:10.1371/journal.pone.0000718.